processes

MDPI

Article

Using Natural Raw Materials and CEM Approach for the Design of Andean Volcanic Self-Compacting Concretes

L. F. Naranjo-Herrera [1], N. M. Páez-Flor [1] and F. J. Rubio-Hernández [2,*]

[1] Departamento de Ciencias de la Energía y Mecánica (DECEM), Universidad de las Fuerzas Armadas—ESPE, Sangolquí 171103, Ecuador
[2] Departamento de Física Aplicada II, Universidad de Málaga, 29071 Málaga, Spain
* Correspondence: fjrubio@uma.es

Abstract: Volcanic activity is characteristic of seismic zones. Consequently, volcanic material form part of the landscape in places where earthquakes are common natural phenomena. As volcanic wastes (VW) show pozzolanic activity, the substitution of manufactured Portland cement (PC) with VW is clearly a desirable option not only from an economical point of view but also to reduce the CO_2 fingerprint. Therefore, designing concretes with volcanic Portland cements (VPC) clearly contributes to cleaner cement production. Construction and building activities in seismic zones need to use a specific kind of concrete—self-compacting concrete (SCC). The challenge we focused on was the design of SCC using VPC. The flow behavior of SCC is characterized by low yield stress, high plastic viscosity, and shear-thickening behavior at high shear. However, obtaining these striking properties of the concrete is not easy with traditional concrete flow tests (Abrams cone, etc.). Moreover, these methods are very costly in terms of time and material. An alternative that allows us to use absolute rheometry and which has been little explored consists in the substitution of concrete by an equivalent mortar. The so-named concrete equivalent mortar (CEM) approach was used in this study to obtain SCC formulations with VPC. Mini cone tests confirmed the absence of blend in some selected CEM formulations based upon the accomplishment of the criteria for SCC. Three concrete proposals were inferred from the respective CEM formulations. They adapted to the SCC European standard according to the Abrams cone spread test.

Keywords: self-compacting concrete; volcanic Portland cement; concrete equivalent mortar

Citation: Naranjo-Herrera, L.F.; Páez-Flor, N.M.; Rubio-Hernández, F.J. Using Natural Raw Materials and CEM Approach for the Design of Andean Volcanic Self-Compacting Concretes. *Processes* **2022**, *10*, 1820. https://doi.org/10.3390/pr10091820

Academic Editor: Jacopo Donnini

Received: 23 August 2022
Accepted: 7 September 2022
Published: 9 September 2022

1. Introduction

Self-compacting concrete (SCC) is a very useful material in building and construction engineering and for its specific application in earthquake resistant structures. Interestingly, the flow behavior of SCC in fresh state is characterized by low yield stress and high plastic viscosity. In addition, shear-thickening behavior is usually observed at relatively high shear [1]. These striking characteristics of SCC result directly from the use of chemical additives (plasticizers). Plasticizers must be compatible with the cementitious phase used in the specific formulation. In addition, the inert solid phase (sand and gravel) must have appropriate geometric features related to its shape, size, and particle size distribution. These components, i.e., chemical additives and inert solid phase, make SCC a material (i) with improved workability, making construction and building activities more efficient; (ii) with better finishing; and (iii) with enhanced manufacturing processes eliminating segregation or bleeding and avoiding the formation of air bubbles. In addition, a valuable property of SCC, especially in earthquake-prone zones, is the possibility to obtain structures with more intricate reinforced concrete, simply because SCC fills formworks much more efficiently.

Seismic and volcanic activities are related phenomena [2–10]. Consequently, natural volcanic wastes (pumice powder (PP) and volcanic ash (VA)) belong to the landscape of

seismic areas. This is very interesting from an economical point of view, because volcanic wastes (VW) show pozzolanic activity and therefore can partially replace Portland cement (PC). This partial substitution of PC by VW gives rise to a new class of cement—the so-called volcanic Portland cement (VPC). This class of cement reduces the CO_2 footprint and cement production costs. It has been also reported that cementitious products that use VPC in their formulation improve physical (cohesiveness, consolidation, flowability, setting time and strength at later ages) and chemical (durability) qualities of concrete [11]. Therefore, the design of SCCs based on VPC (SCCVPC) is clearly an attractive prospect in cleaner production and in safer building for earthquake zones.

The selection of appropriate plasticizers and an inert phase is mandatory for a valid SCCVPC design. We have studied elsewhere [12] the compatibility of several copolymer and lignosulfonate-based plasticizers with a VPC. The VPC used in that study consisted of a mixture of 20 wt% of Andean VW and 80 wt% of pure PC. We say pure PC because the PC was obtained from clinker grinding without any other addition. Only fresh cement pastes formulated with copolymer plasticizers exhibited shear-thickening behavior at high shear rates [12], which is one of the features of SCCs. Therefore, we have assumed in this study the use of this kind of plasticizers for the formulation of SCCVPC.

Empirical techniques (Abrams cone, V-funnel, etc.) have shown limited effectivity for the rheological characterization of SCCs. Fortunately, rheometric techniques that result from the use of absolute rheometers allow researchers a deeper and wider knowledge of the mechanical response of fresh SCCs. However, absolute rheometry can be used only if suspended particles have a very limited maximum size. The maximum particle size must be at least 10 times lower than the gap existing between the solid walls of rheometer geometries. The maximum gap in absolute rheometer geometries is around 1–2 mm for plate–plate, 1–5 mm for concentric cylinder geometries, and only a few microns for the cone–plate geometry, which are the most popular geometrical configurations used with absolute rheometers. Therefore, it is not apparently possible to develop rheometric studies of concretes with absolute rheometers, simply because of the high particle size (as large as ~20 mm) that can be found in concretes. To overcome this drawback, a new methodology has been proposed [13]. It consists of the substitution of the inert phase (sand and gravel) by certain amount of small sand that must have the same total surface area and composition as the original inert phase, but with a maximum particle size compatible with the condition before described for the use of absolute rheometers. This approach is named the concrete equivalent mortar (CEM) methodology [13]. Therefore, the use of the CEM instead of the corresponding concrete eliminates the inconveniences caused by handling coarse aggregates. Other authors [14] have validated the design of SCCs from rheological and mechanical properties of the mortar, i.e., the SCC after the elimination of the coarse aggregate. Note that the principle of CEM is different according to the use of the mortar. The CEM method consists of designing a mortar starting from a certain concrete composition with the objective to study its rheological behavior in a deeper way. Alternatively, and with a clearly different motivation, the rheological study of CEMs aims to obtain specific concrete formulations.

The design of a CEM is based on two hypotheses: (i) the hydration products appear at the interface existing between cement particles and inert solids and (ii) the friction phenomena when the cementitious material flows occur just at that interface. In other words, the total area of the inert aggregates is the fundamental variable to understand the level of workability or, more widely, the rheological behavior of concretes [15]. Therefore, the composition of a CEM is obtained imposing the following conditions with respect to the corresponding concrete. First, the kind and dosage of cement and mineral additives must match. Second, the water/cement (w/c) ratio must coincide. Third, the percentage of additive with respect to the cement amount and the mixing method must be the same. Fourth, the amount of fine aggregate in the CEM must have an identical surface area to that calculated from the total amount of the inert phase (sand and gravel) present in the concrete [13,16].

The aim of this research is to obtain an SCCVPC formulation that is valid for use in building and construction activities at the well-known Ecuadorian seismic zone. For that, we use Ecuadorian sands and commercial VPC formulated with raw VW extracted from Andean volcanos and the CEM approach, with the latter used to confirm the accomplishment of the three specific characteristics of SCCs pointed out above.

2. Theoretical Background

2.1. Multiscale Theory

Multiscale theory predicts the mechanical properties of heterogeneous mixtures from the combined knowledge of the continuous (or dispersant matrix) and its corresponding inclusions (or dispersed phase) [17–20]. When the multiscale theory applies to CEM, the cement paste (cement, water, and chemical additives) is the matrix, and the sand is the dispersed phase. Consequently, we expect that the rheological properties of cement pastes joined to the shape, size, and volume fraction occupied by sand can predict the rheological properties of the CEM. Extending the multiscale theory purpose for the study of concretes, the mortar is the dispersant, and gravel is the dispersed phase. This scheme is certainly attractive when we are thinking of an easier way to design concretes with different practical applications. However, these good prospects must be considered with caution. For example, the results look inappropriate [21] when the prediction of the rheological behavior of a concrete is based upon the rheological behavior of the cement paste, considered as the dispersant phase, and sand and gravel, considered as dispersed phases. This negative result is probably because the rheology of both materials rests on some different grounds. Certainly, while colloidal forces mainly govern the rheology of cement pastes, more complex processes related to friction play a dominant role in the rheological behavior of concretes [22,23]. Therefore, in relation to concrete rheology, the interest in the study of cement paste rheology must be basically reduced to the compatibility and effect of additives. It is necessary to include the inert phase in the arena to obtain wider, deeper, and more realistic knowledge of concrete rheology. According to Schwartzentruber and Catherine [13], this is possible using the CEM methodology. This approach was assumed here.

2.2. Constitutive Equation

It is worthwhile to note that cementitious materials are viscoplastic in nature. This is a widely and well-established behavior observed in all cement-based materials. This mainly means that a threshold stress value, named the yield stress (τ_y), must be necessarily surpassed to observe the flow of fresh cement pastes, mortars, or concretes. Therefore, for viscoplastic materials, the general form of the relationship between shear stress (τ) and shear rate ($\dot{\gamma}$) when $\tau > \tau_y$ must be

$$\tau = \tau_y + f(\dot{\gamma}) \quad (1)$$

where $f(\dot{\gamma})$ is some function of the shear rate. The list of expressions for the function $f(\dot{\gamma})$ is large. One often used expression is $f(\dot{\gamma}) = K\dot{\gamma}^n$. This is the proposal of Herschel and Bulkley (HB equation). However, the use of the HB equation involves two clear disadvantages. First, the HB equation overestimates the yield stress value when the material shows shear-thickening behavior ($n > 1$) because the slope of the flow curve (τ vs. $\dot{\gamma}$) tends to zero at very low shear rates and underestimates the yield stress value when the material shows shear-thinning behavior ($n < 1$) because the slope of the flow curve tends to infinity at very low shear rates. Second, it is not possible to compare different values of the K parameter of different materials due to its "strange" unities ($Pa \cdot s^n$) because, in general, the flow index n will be different for different materials. However, this last inconvenience can be partially bypassed considering that $log\tau$ vs. $log\dot{\gamma}$ plots are commonly used to extract information from steady flow curves. So, from the HB equation, we can obtain that $log(\tau - \tau_y) = logK + nlog\dot{\gamma}$. As $log1 = 0$, $log(\tau_1 - \tau_y) = logK$ when

$\tau_1 = \tau(\dot{\gamma} = 1\ s^{-1})$. Consequently, the comparison between different materials based on $logK$-values acquires some meaning.

Returning to the analysis of Equation (1), it is worth noting that Feys et al. [24] pointed out three conditions that a good viscoplastic equation should always meet. First, the yield stress must be a positive value due to evident physical reasons. Second, it should contain a positive linear term in the shear rate to avoid zero or even negative slope at low shear rates. Third, all parameters of the model should have proper dimensions to allow comparison and physical interpretation of the results. The simplest model that meets these three basic conditions is the second order extension of the linear Bingham model:

$$\tau = \tau_y + \eta_p\dot{\gamma} + c\dot{\gamma}^2 \quad (2)$$

where η_p is the plastic viscosity and c is a second-order coefficient with well-defined unities. It is worthwhile to note that some physical and practical meaning could be tentatively ascribed to the three parameters that appear in Equation (2). First, the yield stress (τ_y) relates to starting flow ability and stability and the resistance to segregation of cementitious materials when they are in an at-rest state [25–27]. Second, the plastic viscosity (η_p) characterizes the pump ability and the resistance to segregation when the material is flowing [28]. Third, as the second-order coefficient (c) value depends on the existence of inclusions–matrix interactions, its value and sign can supply information on the complexity of the viscoplastic behavior, which manifests as a non-linear dependence of the shear stress with the shear rate [29–31].

3. Materials and Methods

3.1. Materials

Three VPCs commercialized by UNACEM (Ecuador), compatible with the Ecuadorian standards INEM 490 [32] and INEM 2380 [33], were used in this study. Table 1 shows chemical and mineralogical compositions of the VPCs, which were obtained by analyzing results of X-ray diffraction obtained with a Panalytical diffractometer (EMPYREAM) and using the High Score Plus software. These cements, under the commercial names Campeón, Selvalegre, and Armaduro, were obtained by the crushing of a mix of clinker and different amounts of natural VW. As expected, the manufacturer does not supply the composition of each VPC. However, thanks to the fact that Andesine, a silicate mineral with pozzolanic activity that is abundant in the Andes Mountains, is the main component of the VW and absent in PC and, on the other hand, alite (C_3S) is absent in VW but is the main phase in PC, we could use the amounts of both andesine and alite to estimate VW and PC amounts in each VPC (Table 1). The Blaine area of the three cements was obtained following NTE INEN 196 norms [34]. The specific density of the cements was obtained following NTE INEN 156 norms [35]. Scanning electron microscopy revealed a similar variety of angular shapes of VPCs particles (Figure 1). In other words, we did not observe significant differences in the particle shape of the three VPCs. SEM micrographs were processed with toolbox routines included in Matlab software (MathWorks Inc., Natick, MA, USA). Similar mean particle sizes (29–32 μm) resulted for the three VPCs. The polydispersity index was 15.5 in all cases, and the specific surface area (BET method) only showed slight variation from one to another VPC (2.2–2.6 m^2/g). Therefore, the amounts of andesine and alite have no influence on the geometric parameters of cement particles, although they have some influence on the rheological behavior of cement pastes [36] and mortars [37].

Table 1. Mineralogical and chemical composition (% wt) of VW and VPCs.

	VW	Campeón	Selvalegre	Armaduro
Andesine	84.00	37.00	36.00	23.00
Tchermakite	8.00	6.40	5.00	4.60
Quartz	3.48	0.80	1.35	1.46
Cordietite	4.30	1.70	0.70	1.30
C_3S	-	40.20	42.70	51.80
C_2S	-	4.90	5.50	6.40
C_4AF	-	2.50	3.10	3.30
C_3A	-	3.80	4.40	5.20
Gypsum	-	2.20	1.70	2.70
VW percentage	100	46.4	42.6	30.6
PC percentage	0	53.6	57.4	69.4
SiO_2	-	34.6	31.4	28.5
Al_2O_3	-	9.5	8.5	7.8
Fe_2O_3	-	4.0	4.1	3.7
CaO	-	42.6	47.9	52
MgO	-	2.4	2.4	2.3
SO_3	-	2.1	2.0	2.3
Na_2O	-	2.0	1.7	1.6
K_2O	-	0.6	0.5	0.5
TiO_2	-	0.5	0.4	0.4
Particle size (μm)	-	29–32	29–32	29–32
Density (g/cm^3)	-	2.94	2.95	3.00
Blaine surface (m^2/g)	-	2.6	2.4	2.2

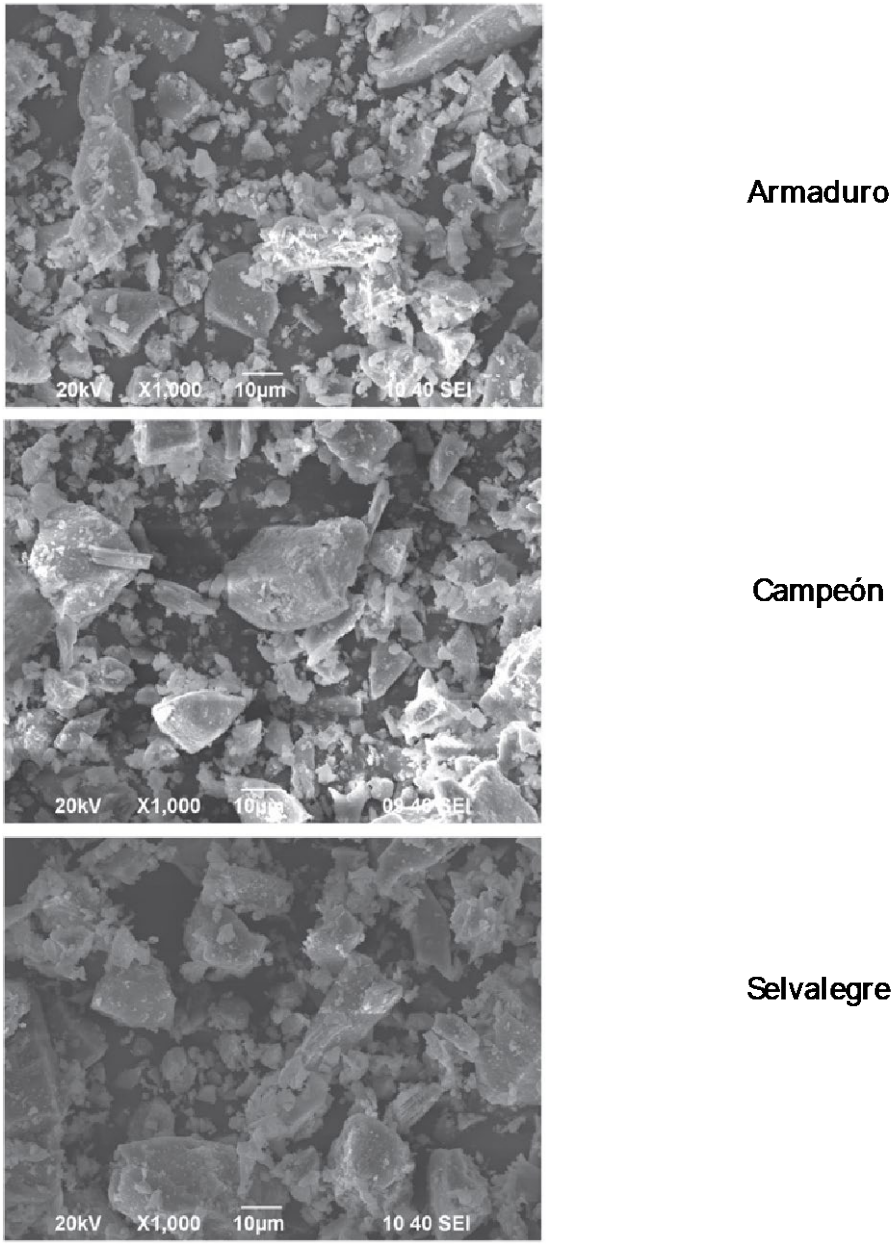

Figure 1. SEM images of VPC particles.

We used sand from three different sources in this study: (i) flushed sand (FS) that came from the volcanoes quarry at the Pintag site, (b) beige sand (BS) extracted from the Pisque quarry of the Guayllabamba site, and (c) blue powder (BP) mined at the Pululahua quarry of the San Antonio de Pichincha site. All these places are in Pichincha (Ecuador). The coarse aggregate came from the Pisque quarry of the Guayllabamba site. The particle size distribution and the density, specific gravity, and absorption percentage of the three sands and coarse aggregate were determined at the Laboratorio de Ensayo de Materiales (Departamento de Ciencias de la Tierra y Construcción, Universidad de las Fuerzas Armadas-ESPE, Ecuador). Results on the particle size distribution are shown in Figure 2. It is worth noting that despite the cumulative passing being similar for the three sands, the particle size distribution is slightly different, which is more clearly shown in Figure 3. As can be seen, the most representative mean particle size, which was obtained using the sieve procedure, followed the sequence $FS(0.20\ mm) < BP(0.22\ mm) < BS(0.42\ mm)$. These three particle size values were used to calculate the sand amount in the corresponding CEM. Monodisperse sands were assumed using this method, which is clearly a source

of error for the calculation of CEM composition. The influence of this assumption on the actual composition of CEMs is probably masked by other error sources, and its quantification is out of the scope of this research. As the shape of sands is a determining factor for the rheological behavior of mortars [38], optical images of the three sands grains were also obtained with a non-polarized light optical microscope (model BA310E, Motic Inc. Ltd., Hong Kong, China). Figure 4 shows that the natural sand (BS) is slightly more spherical than sands obtained by the crushing process (BP, FS), which presumably must facilitate both CEMs and concrete flow ability.

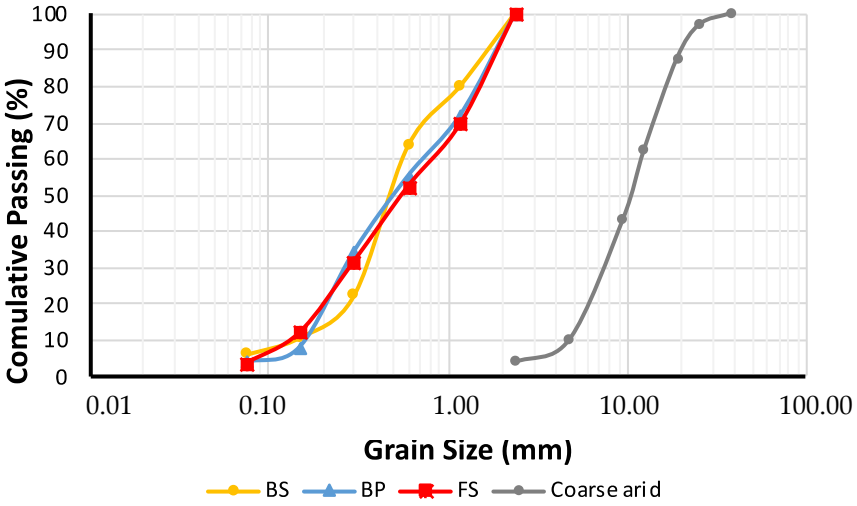

Figure 2. Cumulative passing of the three sands and coarse aggregate.

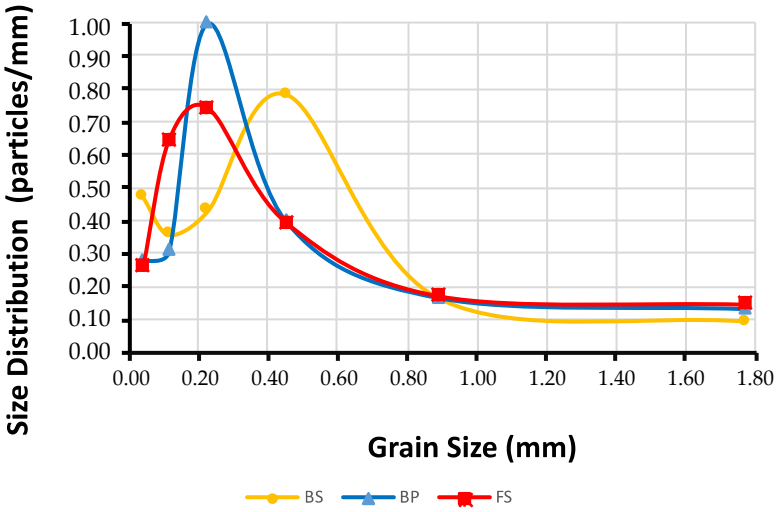

Figure 3. Normalized size distribution of the three sands.

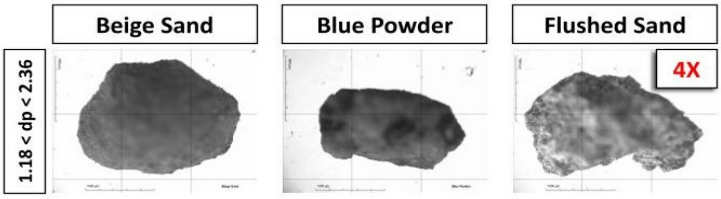

Figure 4. Representative sands grains images obtained with optical microscopy.

To obtain the composition of a mortar, it is mandatory to determine previously the water demand of sand [39]. We obtained the density and water demand of the three sands following NTE INEN 856 and ASTM C128 standards [40]. The densities of the three sands were very similar—specifically, 2.607 g/cm^3 (BS), 2.674 g/cm^3 (BP), and 2.640 g/cm^3 (FS). Water adsorption indexes of natural or crushed sands were 3.5% (BP), 4.0% (BS), and 4.4% (FS). In a nutshell, only the maximum grain size and its shape are parameters that must be eventually used to distinguish the effect of the three sands on the rheological behavior of the CEMs.

Although there are a wide variety of additives, the most widely used for SCC are high-range water reducers and viscosity modifying or cohesive agents. According to the results that we previously obtained [12], copolymer plasticizers show good compatibility with Andean VPCs. Consequently, we focused on commercial copolymer plasticizers to obtain self-compacting characteristics of CEM formulations. Some properties of the additives directly supplied by manufacturers are shown in Table 2.

Table 2. Chemical additives supplied by three different manufacturers.

	ADITEC			**ADMIX**		**SIKA**	
	Techniflow605	**SF106**	**200R**	**Megamix**	**Viscomix**	**Vicocrete 4100**	**Viscoflow50L**
Density (g/cm^3)	1.10	1.18	1.19	1.17	1.07	1.10	1.11
Dosage interval (%)	0.19–0.9	0.93–2	0.93–2	0.5–2.5	0.5–1.5	0.19–0.9	0.4–2.3

3.2. Protocols

The design of protocols for rheological experimentation with fresh cementitious materials must consider the necessity to minimize the influence on the results of the cement hydration process. In addition, it is mandatory to define the mechanical reference state of the fresh cementitious slurry well to ensure the repeatability of the experimental results. In line with these ideas, the time interval from cement/water first contact to the end of the rheological test must be lower than the induction period of the cement, which is typically around 30 min. Moreover, it is worthwhile to note that the resting state favors the hydration of the cement. Consequently, it is convenient to design the steady flow curve (SFC), a rheological test that records the steady stress response of the material to a series of shear rates monotonously distributed, starting from the higher shear rate value. Therefore, the SFC corresponding to each sample was the plot of the steady shear stress versus the shear rate value monotonously distributed in a decreasing ramp of shear rates from 120 s^{-1} to 1 s^{-1}, as shown in Figure 5. It is also worthwhile to note that each shear rate was applied during the time necessary to record the steady shear stress response. Only when the relative variation of the stress response to each shear rate was less than 5% for 20 s was the accomplishment of steady condition assured. We present the results of SFCs as the average value of three measurements taken with three different samples of the same cementitious slurry (3 × 3 = 9) measurements. Finally, and related to the design of the SFC protocol, it is worthwhile to note that random stresses can develop in samples during mixing and handling processes that take place in the preparation and positioning of samples before the measuring procedures. Therefore, a pre-shear phase that consisted in the application

of the maximum shear (120 s^{-1}) during 60 s was included before the rheological testing to erase undesirable random effects.

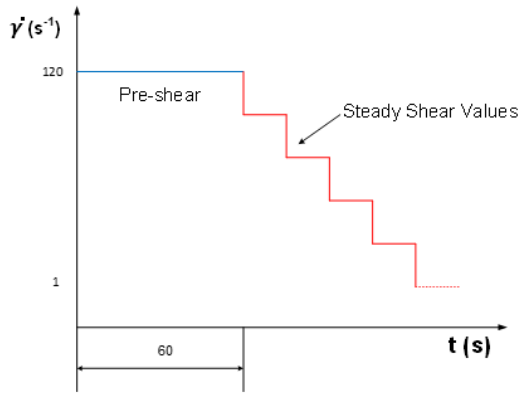

Figure 5. Steady flow curve protocol.

In the case of cementitious materials, a well-defined protocol for the preparation of samples is mandatory. The preparation protocol has a determinant influence on the rheological behavior of cementitious materials. We prepared all samples as follows. The liquid phase (water and additive) was added to the previously mixed dry phase (cement and sand). A Hamilton Beach 64650 mixer (Hamilton Beach Brands, Inc., Glen Allen, VA, USA) was used to mix the components for 10 min at a constant velocity of 540 rpm. A damp cloth covered the mixture to prevent water evaporation and cement scab formation. The geometry selected for the mixing was a spindle of spans. The distance between the base of the container and the lower base of the spindle was 3500 μm.

3.3. CEMs Design

For the design of CEMs, we followed the method described in detail in [16]. We selected a concrete formulation normalized according to the recommendation of Colegio Oficial de Ingenieros Civiles (Quito, Ecuador) as referenced concrete. It indicates the general amounts of cement, sand, gravel, and water used in concretes for civil applications in Ecuador (Table 3).

Table 3. Composition of a normalized Ecuadorian concrete.

Cement (kg)	Sand (kg)	Gravel (kg)	Water (kg)
520	750	750	208

The specific surface area of the aggregates and the amount of water in the concrete are the two main critical parameters to be calculated for the design of the corresponding CEM. The data and calculations needed to obtain the specific surface area of the three sands and gravel used in this study are shown in Tables 4 and 5, respectively.

Table 4. Specific surface area of the three sands.

BS				BP			FS		
Sieve (mm)	**Cumulative Passing (%)**	**S (m^2)**	**Weighted Surface (m^2/kg)**	**Cumulative Passing (%)**	**S (m^2)**	**Weighted Surface (m^2/kg)**	**Cumulative Passin (%)**	**S (m^2)**	**Weighted Surface (m^2/kg)**
<0.075	0.00	65.17	4.039	0.00	63.19	2.337	0.00	64.86	2.209
0.075	6.20	21.82	1.013	3.70	21.16	0.844	3.41	21.72	1.823
0.149	10.84	10.88	1.242	7.69	10.56	2.793	11.80	10.83	2.133
0.3	22.25	5.43	2.234	34.15	5.27	1.101	31.49	5.40	1.121
0.6	63.42	2.74	0.459	55.06	2.66	0.454	52.23	2.73	0.477
1.18	80.16	1.38	0.274	72.11	1.34	0.373	69.70	1.37	0.416
2.36	100.00	0.77	0.000	100.00	0.75	0.000	100.00	0.76	0.000
			9.261			7.902			8.179

Table 5. Specific surface area of the gravel.

Sieve (mm)	**Cumulative Passing (%)**	**S (m^2)**	**Weighted Surface (m^2/kg)**
<2.36	0.00	2.097	0.079
2.36	3.76	0.695	0.044
4.76	9.93	0.347	0.115
9.51	43.19	0.225	0.043
12.5	62.49	0.157	0.039
19	87.51	0.111	0.010
25.4	96.92	0.079	0.002
38.1	100.00	0.055	0.000
			0.332

The number of particles (N) in 1 kg of aggregate was calculated from Equation (3), where ρ_s (kg / m^3) is the sand density and D (m) the equivalent diameter of the grain. The specific surface area S corresponding to each grain size was obtained with Equation (4). Therefore, the specific surface area of an aggregate is the sum of the specific surface area of all grain sizes, i.e., 9.261 m^2/kg (BS), 7.902 m^2/kg (BP), 8.179 m^2/kg (FS), and 0.331 m^2/kg (gravel).

$$\boldsymbol{N = \frac{Total\ volume}{Particle\ volume} = \frac{\frac{1}{\rho_s}}{\frac{4}{3}\pi\left(\frac{D}{2}\right)^3}} \quad (3)$$

$$\boldsymbol{S = N\pi D^2} \quad (4)$$

Knowing the specific surface area of each aggregate, the amount of sand required for the design of the CEM ($M_{sand\ CEM}$) was calculated with Equation (5):

$$\boldsymbol{M_{sand\ CEM} = m_{sand\ C} + \frac{m_{gravel\ C} \times S_{gravel}}{S_{sand}}} \quad (5)$$

where $m_{sand\ C}$ and $m_{gravel\ C}$ are, respectively, the amount of sand and gravel in the original concrete, and S_{sand} and S_{gravel} are the specific surface area of sand and gravel, respectively.

The total amount of water needed for a CEM preparation (M_{water}) must be calculated considering not only the proposed *w*/*c* ratio (first term in Equation (6)), but also the water absorbed by the sand (second term in Equation (6)) and the water amount directly provided by the additive (third term in Equation (6)), i.e.,

$$\boldsymbol{M_{water} = \frac{w}{c}M_{cement} + \frac{M_{sand\ CEM}}{1 + \frac{Absorption\ coefficient}{100}}\frac{Absorption\ coefficient}{100} - M_{additive}\frac{1 - Dry\ residue}{100}} \quad (6)$$

Finally, the composition of the different CEMs rheologically tested in this study are shown in Table 6. The effect of the fineness of sand in the rheological behavior of a given CEM was also studied, dividing the total amount of sand in three different maximum particle sizes. Therefore, F1 corresponds to sand passing a sieve of 2.36 mm, F2 includes only sand passing a sieve of 0.30 mm, and, finally, F3 contains sand with the maximum size of 0.149 mm (see the last column in Table 6).

Table 6. Composition of the different CEMs.

Cement	Sand	Sand/Cement (s/c)	Water/Cement (*w*/*c*)	Additive (%)	Fi/Cement (Fi/c)
SA	BS	1.49	0.30	2.00	1.49 (F1)
			0.35		1.03 (F2)
			0.40		0.34 (F3)
	BP	1.75	0.30		1.75 (F1)
			0.35		1.08 (F2)
			0.40		0.49 (F3)
	FS	1.69	0.30		1.69 (F1)
			0.35		0.99 (F2)
			0.40		0.41 (F3)
CO	BS	1.49	0.30	2.00	1.49 (F1)
			0.35		1.03 (F2)
			0.40		0.34 (F3)
	BP	1.75	0.30		1.75 (F1)
			0.35		1.08 (F2)
			0.40		0.49 (F3)
	FS	1.69	0.30		1.69 (F1)
			0.35		0.99 (F2)
			0.40		0.41 (F3)
AM	BS	1.49	0.30	2.00	1.49 (F1)
			0.35		1.03 (F2)
			0.40		0.34 (F3)
	BP	1.75	0.30		1.75 (F1)
			0.35		1.08 (F2)
			0.40		0.49 (F3)
	FS	1.69	0.30		1.69 (F1)
			0.35		0.99 (F2)
			0.40		0.41 (F3)

3.4. Equipment

A controlled stress rheometer (DHR-2, TA Instruments, New Castle, DE, USA) was used for the rheological testing. This device was equipped with a Peltier system for the temperature control. A four-vane geometry was used. The advantage of the use of a vane rotor with cementitious materials has been extensively justified [41]. The diameter of the rotor was 28.0 ± 0.1 mm, and its height was 42.0 ± 0.1 mm. The rotor was introduced in a concentric cylinder (stator) with an inner diameter of 30.0 ± 0.1 mm for cement pastes (1 mm gap), and in a similar concentric cylinder with an inner diameter of 40.0 ± 0.1 mm for mortar mixes (6 mm gap).

4. Results and Discussion

4.1. Selecting the Additive to Be Used in CEMs Formulation

The effect of the type and amount of additive on the SFC of Armaduro cement pastes ($0.35\ \%w/c$) is shown in Figure 6. The amount of additive was calculated with respect to the cement weight (%cw). Results for Armaduro cement paste without any additive, labeled as Armaduro 0%, are also included for comparison. Results obtained with the two other cements (Selvalegre and Campeón) are not shown to avoid unnecessary repetition because, qualitatively speaking, the results were very similar. No matter which recommendations of the fabricant were used (see Table 2), cement pastes with the proportions $1, 2,$ and 3 %cw of the additives were tested.

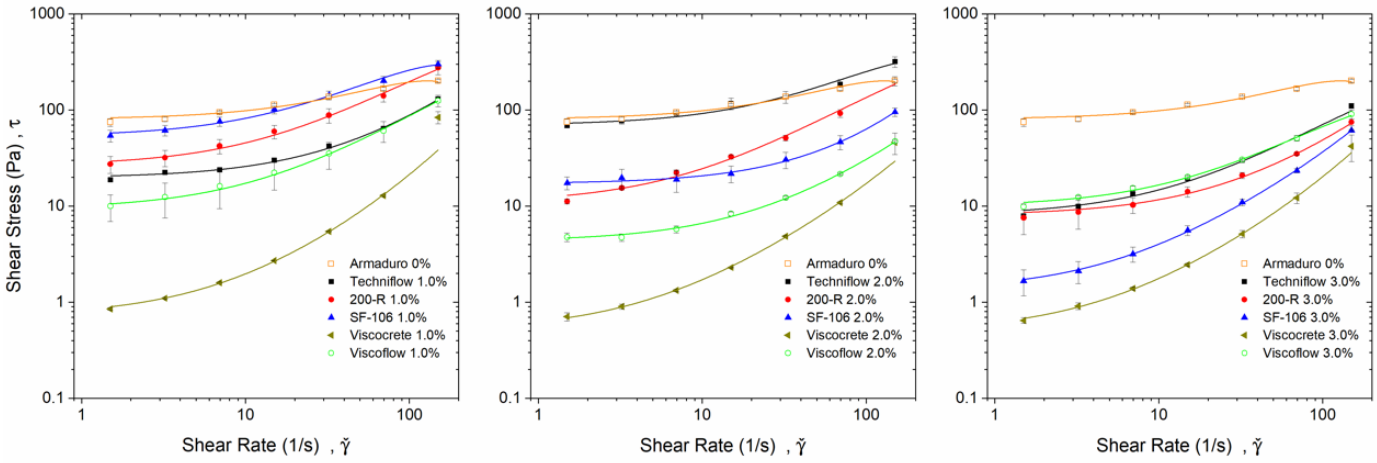

Figure 6. Effect of additive type and amount on SFCs of Armaduro cement pastes.

Quantitatively speaking, to achieve self-compacting characteristics of the cement paste, the higher the plastic viscosity and the lower the yield stress, the better the effect of the additive. Results of the SFC shown in Figure 6 were fitted with the modified Bingham equation. The values of the modified Bingham parameters are shown in Table 7. As can be seen, the modified Bingham model fitted very well to experimental points ($R^2 \geq 0.9994$). The additive Viscocrete supplied lower yield stress values. It is worthwhile to remind readers that low values of the yield stress indicate that the cementitious material can flow more easily by its own weight, which is one well-appreciated self-compacting characteristic. An additional decrease of the yield stress value was achieved when the Viscocrete dosage increased from 1 %cw to 2 %cw. The yield stress did not decrease anymore when the amount of Viscocrete increased to 3 %cw. Consequently, 2 %cw was the additive dosage finally accepted for the rest of the research. Unfortunately, the value of the plastic viscosity was not the highest when Armaduro cement paste contains the Viscocrete additive. This means that probably with the use of this additive, some bleeding of the cementitious slurry must be observed. Alternatively, for example, the Viscoflow additive supplied higher plastic viscosity values, which is a positive result to avoid the bleeding of the paste; however, the yield stress values were more than 10 times higher than those obtained with the use of Viscocrete. To decide on the more appropriate additive according with the aim of this research, the third characteristic of SSC, i.e., shear-thickening behavior at high shear rates [1], was considered. This rheological behavior manifests in positive values of the second-order coefficient of the modified Bingham model. As can be seen in Table 7, this was the case with the additive Viscocrete.

Table 7. Parameters of modified Bingham equation. Effect of additives on Armaduro CP $(0.35\ \%\ w/c)$.

Additive	% cw	R^2	$\tau_{MB}\ (Pa)$	$\eta_p\ (Pa.s)$	$c\ (Pa.s^2)$
Techniflow	1	0.9997	20 ± 1	0.60 ± 0.05	0.0008 ± 0.0003
	2	0.9998	70 ± 4	2.3 ± 0.5	~ 0
	3	0.9995	8.1 ± 0.9	0.68 ± 0.06	~ 0
200-R	1	0.9999	27 ± 7	1.9 ± 0.2	~ 0
	2	0.9996	9.5 ± 0.8	1.5 ± 0.1	$-(0.002 \pm 0.001)$
	3	0.9999	8.0 ± 0.6	0.35 ± 0.03	~ 0
SF 106	1	0.9994	53 ± 9	3.0 ± 0.3	$-(0.009 \pm 0.002)$
	2	0.9999	17.2 ± 0.5	0.34 ± 0.04	0.0010 ± 0.0003
	3	0.9999	1.3 ± 0.1	0.26 ± 0.01	0.0009 ± 0.0001
Viscocrete	1	0.9997	0.7 ± 0.2	0.12 ± 0.02	0.0009 ± 0.0004
	2	0.9999	0.52 ± 0.08	0.12 ± 0.01	0.0005 ± 0.0002
	3	0.9999	0.50 ± 0.04	0.12 ± 0.01	0.0008 ± 0.0001
Viscoflow	1	0.9999	8.8 ± 0.3	0.83 ± 0.06	~ 0
	2	0.9999	4.3 ± 0.2	0.23 ± 0.01	0.0004 ± 0.0001
	3	0.9999	9.9 ± 0.5	0.68 ± 0.04	$-(0.0011 \pm 0.0005)$
-	0	0.9995	80 ± 4	1.9 ± 0.2	$-(0.007 \pm 0.001)$

4.2. Rheological Behavior of the F1-CEMs

The effects of cement type, w/c ratio, and sand type on the SFC of F1-CEMs were studied. The modified Bingham model (Equation (2)) was fitted to the experimental data, and the resulting model parameters are shown in Table 8.

Table 8. Parameters of modified Bingham equation. F1-CEMs.

Cement	Aggregate	w/c	$\tau_{MB}\ (Pa)$	$\eta_p\ (Pa.s)$	$c\ (Pa.s^2)$	R^2
Selvalegre	BS	0.30	28 ± 2	16.6 ± 0.3	$-(0.43 \pm 0.08)$	0.9930
		0.35	25 ± 2	9.2 ± 0.5	$-(0.08 \pm 0.01)$	0.9979
		0.40	10 ± 2	5.7 ± 0.1	$-(0.047 \pm 0.002)$	0.9999
	BP	0.30	33 ± 3	26 ± 1	$-(0.32 \pm 0.03)$	0.9983
		0.35	26 ± 1	12.5 ± 0.4	$-(0.091 \pm 0.009)$	0.9995
		0.40	20 ± 1	7.8 ± 0.2	$-(0.070 \pm 0.006)$	0.9994
	FS	0.30	30 ± 1	13.4 ± 0.1	$-(0.146 \pm 0.002)$	0.9970
		0.35	25 ± 1	8.2 ± 0.1	$-(0.080 \pm 0.001)$	0.9980
		0.40	12 ± 1	4.2 ± 0.3	$-(0.033 \pm 0.006)$	0.9982
Campeón	BS	0.30	30 ± 2	17 ± 1	$-(0.19 \pm 0.02)$	0.9988
		0.35	25 ± 1	10 ± 1	$-(0.089 \pm 0.008)$	0.9992
		0.40	15 ± 1	7 ± 1	$-(0.062 \pm 0.005)$	0.9994
	BP	0.30	35 ± 2	27.0 ± 0.9	$-(0.29 \pm 0.02)$	0.9989
		0.35	30 ± 2	13.2 ± 0.8	$-(0.08 \pm 0.02)$	0.9979
		0.40	20 ± 1	7.8 ± 0.4	$-(0.07 \pm 0.01)$	0.9981
	FS	0.30	30 ± 2	14.3 ± 0.7	$-(0.12 \pm 0.02)$	0.9985
		0.35	20 ± 1	8.5 ± 0.3	$-(0.072 \pm 0.006)$	0.9995
		0.40	10 ± 1	4.4 ± 0.2	$-(0.033 \pm 0.004)$	0.9993
Armaduro	BS	0.30	20 ± 1	16.4 ± 0.2	$-(0.151 \pm 0.003)$	0.9999
		0.35	10 ± 1	5.6 ± 0.2	$-(0.019 \pm 0.003)$	0.9980
		0.40	8 ± 1	2.5 ± 0.2	$-(0.007 \pm 0.002)$	0.9960
	BP	0.30	25 ± 1	16.3 ± 0.4	$-(0.13 \pm 0.01)$	0.9995
		0.35	20 ± 1	7.8 ± 0.4	$-(0.032 \pm 0.004)$	0.9979
		0.40	15 ± 1	4.3 ± 0.2	$-(0.018 \pm 0.003)$	0.9974
	FS	0.30	25 ± 1	8.8 ± 0.3	$-(0.080 \pm 0.007)$	0.9994
		0.35	15 ± 1	4.3 ± 0.3	$-(0.015 \pm 0.003)$	0.9966
		0.40	7 ± 1	2.1 ± 0.1	$-(0.007 \pm 0.001)$	0.9985

The sign of the second-order coefficient is negative in all cases, which indicates that the presence of F1-sand eliminates the expected shear-thickening behavior obtained when Viscocrete additive was used in CP formulations. This must be presumably because the presence of F1-sand reduces the adsorption capability of copolymer molecules on cement particles. On the other hand, the yield stress diminishes when the w/c ratio increases. This is an expected result because higher water content must give rise to an increase of the mortar fluidity. On the other hand, no significative differences in yield stress and plastic viscosity values were obtained using different VPCs. Therefore, F1-CEMs formulated with the three VPCs should flow and bleed similarly. This conjecture could be confirmed by the inspection of mini-cone results shown in Figure 7 because, as can be seen, no appreciable differences in size and bleeding of the three slump tests could be detected.

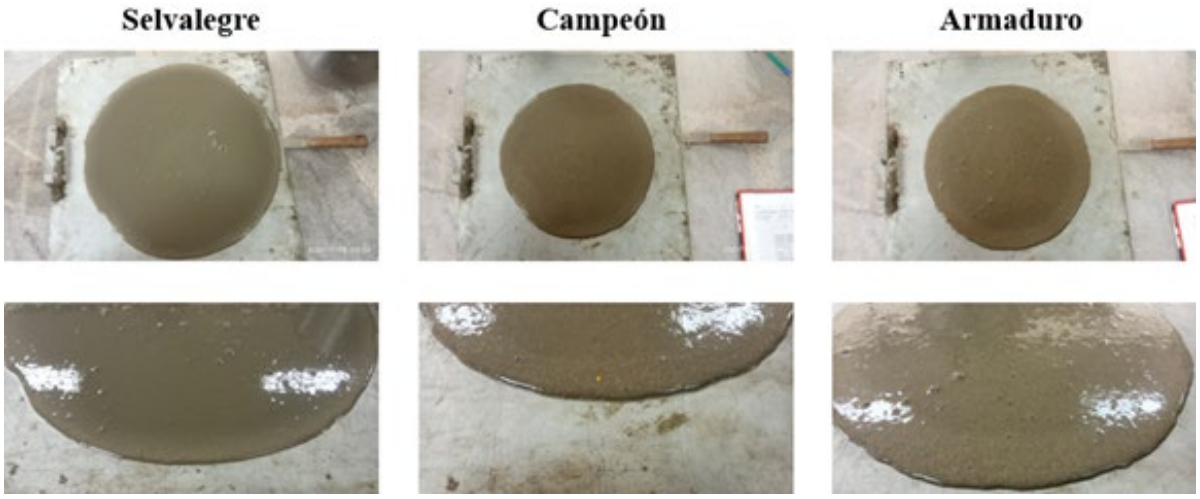

Figure 7. F1-CEM mini-cone results. BS sand. $w/c = 0.30$. 2.0 %cw Viscocrete.

To improve the performance of VPCs as basic components in SCC formulations, we tested the influence of sand fineness on the modified Bingham model parameters, especially with the objective of detecting possible changes in the sign of the second-order coefficient.

4.3. Rheology of F2-CEMs and F3-CEMs

The fineness of sands was reduced while maintaining the sand type and the total specific surface area as constant. Therefore, in addition to F1-CEMs, we also studied equivalent mortars labeled as F2-CEMs and F3-CEMs. While F2-CEMs are equivalent mortars with a maximum sand particle size of 0.30 mm, F3-CEMs correspond to equivalent mortars with a maximum sand particle size of 0.149 mm (see Table 4 for interpretation of F1, F2, and F3 nomenclature).

The parameters of the modified Bingham equation fitted to the experimental data corresponding to F2-CEMs and F3-CEMs SFC are shown in Tables 9 and 10. As can be seen, the sign of the second-order parameter changes from negative to positive when the fineness of sand diminishes. The overall conclusion is that the effectivity of Viscocrete additive to maintain separated cement particles increases when sand particles are smaller. In this way, we can observe shear-thickening behavior at high shear rates with some F3-CEMs. In addition, particles with a smaller size must favor CEM flow, acting as effective bearings. This is consistent with the fact that yield stresses are lower with F3-CEMs than with F2-CEMs and, in this last case, are lower than with F1-CEMs.

Table 9. Parameters of modified Bingham equation. F2-CEMs.

Cement	Aggregate	w/c	τ_{MB} (Pa)	η_p $(Pa.s)$	c $(Pa.s^2)$	R^2
Selvalegre	BS	0.30	15 ± 2	12 ± 1	$-(0.11 \pm 0.02)$	0.9942
		0.35	5.0 ± 0.2	4.30 ± 0.08	$-(0.027 \pm 0.002)$	0.9998
		0.40	5.4 ± 0.4	1.30 ± 0.01	$-(0.004 \pm 0.001)$	0.9986
	BP	0.30	3.0 ± 0.2	3.9 ± 0.4	~ 0	0.9941
		0.35	0.8 ± 0.2	0.83 ± 0.01	0.021 ± 0.001	0.9998
		0.40	0.9 ± 0.3	0.34 ± 0.01	0.007 ± 0.001	0.9993
	FS	0.30	10 ± 2	11.9 ± 0.6	$-(0.12 \pm 0.01)$	0.9977
		0.35	4.0 ± 0.2	3.8 ± 0.1	~ 0	0.9995
		0.40	2.5 ± 0.1	1.03 ± 0.05	~ 0	0.9984
Campeón	BS	0.30	9 ± 2	9.5 ± 0.5	$-(0.07 \pm 0.01)$	0.9976
		0.35	6.0 ± 0.3	5.2 ± 0.2	$-(0.025 \pm 0.005)$	0.9992
		0.40	3.0 ± 0.1	1.20 ± 0.05	~ 0	0.9988
	BP	0.30	15 ± 2	18 ± 1	$-(0.21 \pm 0.03)$	0.9957
		0.35	5.0 ± 0.2	5.7 ± 0.7	~ 0	0.9919
		0.40	3.0 ± 0.1	2.48 ± 0.06	~ 0	0.9994
	FS	0.30	12 ± 1	1.14 ± 0.09	0.025 ± 0.003	0.9972
		0.35	6.0 ± 0.2	1.1 ± 0.3	$-(0.025 \pm 0.009)$	0.9984
		0.40	2.5 ± 0.1	0.97 ± 0.03	~ 0	0.9992
Armaduro	BS	0.30	7.0 ± 0.3	5.8 ± 0.1	$-(0.018 \pm 0.002)$	0.9994
		0.35	2.5 ± 0.1	1.84 ± 0.03	0.004 ± 0.001	0.9998
		0.40	2.5 ± 0.1	1.02 ± 0.02	~ 0	0.9998
	BP	0.30	6.0 ± 0.2	7 ± 1	~ 0	0.9866
		0.35	2.5 ± 0.1	2.04 ± 0.06	0.008 ± 0.001	0.9993
		0.40	2.4 ± 0.2	0.45 ± 0.04	~ 0	0.9967
	FS	0.30	5.0 ± 0.3	4.9 ± 0.1	$-(0.007 \pm 0.001)$	0.9990
		0.35	2.5 ± 0.1	1.58 ± 0.03	~ 0	0.9997
		0.40	2.3 ± 0.1	0.63 ± 0.04	0.003 ± 0.001	0.9977

Table 10. Parameters of the modified Bingham equation. F3-CEMs.

Cement	Aggregate	w/c	τ_{MB} (Pa)	η_p $(Pa.s)$	c $(Pa.s^2)$	R^2
Selvalegre	BS	0.30	1.0 ± 0.1	1.1 ± 0.2	0.026 ± 0.004	0.9999
		0.35	0.80 ± 0.03	0.32 ± 0.02	0.013 ± 0.001	0.9992
		0.40	0.35 ± 0.01	0.15 ± 0.01	0.005 ± 0.001	0.9996
	BP	0.30	15 ± 1	20 ± 2	$-(0.29 \pm 0.06)$	0.9904
		0.35	7 ± 1	8.4 ± 0.8	$-(0.05 \pm 0.02)$	0.9925
		0.40	4 ± 1	2.28 ± 0.06	$-(0.005 \pm 0.001)$	0.9993
	FS	0.30	1.5 ± 0.1	0.98 ± 0.09	0.025 ± 0.003	0.9965
		0.35	1.4 ± 0.1	0.42 ± 0.02	0.010 ± 0.001	0.9991
		0.40	0.45 ± 0.01	0.13 ± 0.01	0.004 ± 0.001	0.9996
Campeón	BS	0.30	2.5 ± 0.1	2.8 ± 0.2	0.03 ± 0.01	0.9971
		0.35	1.3 ± 0.1	0.64 ± 0.06	0.013 ± 0.002	0.9962
		0.40	1.0 ± 0.3	0.27 ± 0.01	0.008 ± 0.001	0.9994
	BP	0.30	2.5 ± 0.1	1.12 ± 0.05	~ 0	0.9916
		0.35	1.3 ± 0.1	0.60 ± 0.01	0.22 ± 0.02	0.9960
		0.40	1.0 ± 0.3	0.24 ± 0.03	0.38 ± 0.01	0.9976
	FS	0.30	9.5 ± 0.1	10.9 ± 0.7	$-(0.09 \pm 0.01)$	0.9961
		0.35	1.3 ± 0.1	0.38 ± 0.02	0.010 ± 0.001	0.9990
		0.40	0.4 ± 0.1	0.11 ± 0.01	0.004 ± 0.001	0.9997
Armaduro	BS	0.30	0.92 ± 0.03	0.46 ± 0.02	0.012 ± 0.001	0.9994
		0.35	0.85 ± 0.02	0.23 ± 0.01	0.007 ± 0.001	0.9996
		0.40	0.25 ± 0.01	0.13 ± 0.01	0.004 ± 0.001	0.9998
	BP	0.30	1.03 ± 0.03	0.76 ± 0.02	0.019 ± 0.001	0.9997
		0.35	1.01 ± 0.04	0.38 ± 0.01	0.007 ± 0.001	0.9989

		0.40	0.31 ± 0.01	0.15 ± 0.01	0.004 ± 0.001	0.9998
		0.30	0.85 ± 0.01	0.51 ± 0.01	0.011 ± 0.001	0.9999
	FS	0.35	0.40 ± 0.01	0.24 ± 0.01	0.005 ± 0.001	0.9999
		0.40	0.37 ± 0.01	0.06 ± 0.01	0.003 ± 0.001	0.9991

4.4. SCCVPC Formulation

Spread tests with an Abrams mini cone were carried out with F1-, F2-, and F3-CEMs (Table 11). As can be seen, the diameter of the spread increases when the size of the sand used for CEM formulations decreases. In addition, the flow time T20, i.e., the period between the moment the mini-cone leaves the base plate and the CEM touches the circle of diameter 20 mm, decreases when the size of sand decreases. The three F3-CEMs showed the best results, i.e., lower yield stress, higher plastic viscosity, positive sign of the second-order parameter, larger spread, and lower T20. Images of spread tests with the three F3-CEMs confirm this statement (Figure 8). Note the absence of bleeding. Therefore, these three F3-CEM formulations were selected to infer the corresponding concrete formulations.

Figure 8. Mini-cone tests of selected F3-CEMs. BS sand. $w/c = 0.30$. 2.0 %cw Viscocrete.

Table 11. Tests using the Abrams mini cone of equivalent mortar detailed in Tables 8–10, with normalized concrete according to the recommendation of Colegio Oficial de Ingenieros Civiles (Quito, Ecuador) was selected (Table 3).

CEM Phase	Cement (kg)	Sand (kg)	Water/Cement (w/c)	2% Additive (kg)	Water Absorption (kg)	T_{20} (s)	d (cm)
F1	SA	BS					
	520.00	751.28	0.30	10.40	31.08	15.54	27.75
	CO	BS					
	520.00	751.28	0.30	10.40	31.08	13.25	28.00
	AM	BS					
	520.00	751.28	0.30	10.40	31.08	8.12	28.00
F2	SA	BS					
	520.00	516.89	0.30	10.40	25.79	7.45	30.75
	CO	BS					
	520.00	516.89	0.30	10.40	25.79	5.10	33.00
	AM	BS					
	520.00	516.89	0.30	10.40	25.79	4.17	32.50
F3	SA	BS					
	520.00	246.43	0.30	10.40	12.22	3.48	38.00
	CO	BS					
	520.00	246.43	0.30	10.40	12.22	3.91	36.75
	AM	BS					
	520.00	246.43	0.30	10.40	12.22	3.21	33.75

The concrete formulations were designed following the recommendations given by Colegio Oficial de Ingenieros Civiles (Quito, Ecuador) (Table 3). As can be seen in Table

12, the flow time T50, i.e., the period between the moment the cone leaves the base plate and the concrete touches the circle with a diameter of 500 mm, and the size of the spread confirm they are SCCs according to the European Guidelines for Self-Compacting Concrete Specification Production and Use (EN 12350-1, 2011; EN 12350-2, 2019). Images of spread Abrams cone tests with the three concretes confirm the absence of bleeding (Figure 9).

Table 12. Concrete formulations inferred from F3-CEMs (Table 11) and the recommendations by Colegio Oficial de Ingenieros Civiles (Quito, Ecuador) (Table 3).

Gravel (kg)	Cement (kg)	Sand (2.36 mm) (kg)	Water/Cement (w/c)	2% additive (kg)	T_{50} (s)	d (cm)
	SA	BS				
750.00	520.00	237.9	0.30	10.40	24.10	86.30
	CO	BS				
750.00	520.00	237.9	0.30	10.40	17.83	88.8
	AM	BS				
750.00	520.00	237.9	0.30	10.40	12.03	93.00

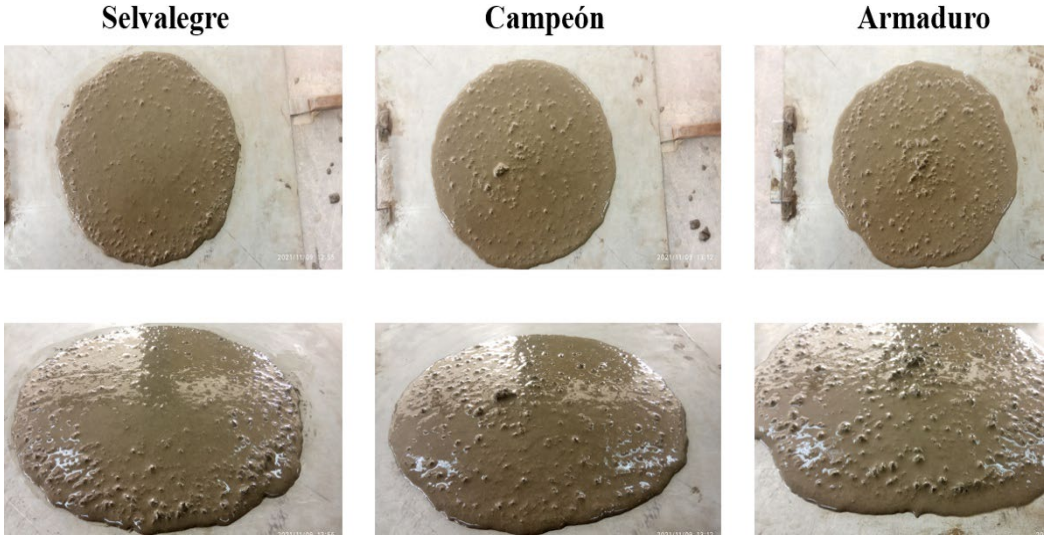

Figure 9. Results of the Abrams cone corresponding to the three SCCVPC inferred from the corresponding F3-CEMs (BS sand, $w/c = 0.30$, 2.0 %cw Viscocrete additive).

5. Conclusions

Building and construction in seismic zones must be resistant against earthquakes. Therefore, more intricate reinforced concrete must be selected. In other words, SCC is indicated in those places. In addition, as volcanic activity is characteristic of seismic zones, huge amounts of natural raw volcanic materials are part of the landscape in seismic zones. As VWs are pozzolanic, they can be used as substitutes for PC, reducing the CO_2 fingerprint and giving economic and social advantage to a natural source, specifically in undeveloped and third-world countries. The objective of this research was to design an SCC using raw VW and sand and cements commercialized in Ecuador. To accomplish this objective, different cements, sands, and additives were considered. Absolute rheological information must be known to determine well-defined self-compacting characteristics, i.e., low yield stress, high plastic viscosity, and shear-thickening behavior at high shear. Therefore, appropriate concrete equivalent cementitious material should be used. Fortunately, the CEM approach was developed in 2000 [13], allowing us to accomplish our goals. Spurred on by the good previous results obtained by using the CEM approach [16], we decided to follow this program to design an SCCVPC. Therefore, the flow behavior of concrete equivalent mortars (CEMs) was tested with an absolute rheometer. Lower yield

stress, higher plastic viscosity, and shear-thickening behavior at high shear were used as signs of self-compacting characteristics of the CEMs. Three concretes were formulated from the CEMs that better achieved self-compacting characteristics. The results of Abrams cone spread tests made with the concretes agreed with the SCC European standard, which was used as an independent test of the validity of our CEM-based results.

The most remarkable conclusion of this work is that the CEM approach can be used to infer SCCVPC formulations.

Author Contributions: Conceptualization, Methodology, Formal analysis, Resources, Data curation, Writing—original draft, Writing—review and editing, Supervision, F.J.R.-H.; Conceptualization, Methodology, Validation, Investigation, Data curation, Writing—original draft, L.F.N.-H. and N.M.P.-F. All authors have read and agreed to the published version of the manuscript.

Funding: This research received no external funding.

Data Availability Statement: The datasets used and/or analyzed during the current study are available from the corresponding author on reasonable request.

Acknowledgments: L.F.N.-H. and N.M.P.-F. thank the Laboratory of Rheology of Department of Energy Sciences and Mechanics of the University of the Armed Forces, ESPE, for allowing the use of the DHR-2 rheometer equipment and the laboratory facilities and support from the work team. We also thank the Materials Testing Laboratory of Earth Sciences and Construction of the University of the Armed Forces, ESPE for technical support.

Conflicts of Interest: The authors declare no conflict of interest.

References

1. Feys, D.;Verhoeven, R.; De Schutter, G. Why is fresh self-compacting concrete shear thickening? *Cem. Concr. Res.* **2009**, *39*, 510–523.
2. Lemarchand, N.; Grasso, J.R. Interactions between earthquakes and volcano activity. *Geophys. Res. Lett.* **2007**, *34*, L24303.
3. Jiménez, M.J.; García-Fernández, M.; Romero, J. 1989–1995 Earthquake sequences in the Galeras volcano region, SW Colombia, and possible volcano-earthquake interactions. *Tectonophysics* **2009**, *463*, 47–59.
4. Higgins, M.D. The Cascadia megathrust earthquake of 1700 may have rejuvenated and isolated basalt volcano in western Canada: Age and petrographic evidence. *J. Volcanol. Geoth. Res.* **2009**, *179*, 149–156.
5. Aoyama, H.; Onizawa, S.; Kobayashi, T.; Tameguri, T.; Hashimoto, T.; Oshima, H.; Mori, H.Y. Inter-eruptive volcanism at Usu volcano: Micro-earthquakes and dome subsidence. *J. Volcanol. Geoth. Res.* **2009**, *187*, 203–217.
6. De la Cruz-Reyna, S.; Tárraga, M.; Ortiz, R.; Martínez-Bringas, A. Tectonic earthquakes triggering volcanic seismicity and eruptions. Case studies at Tungurahua and Popocatépetl volcanoes. *J. Volcanol. Geoth. Res.* **2010**, *193*, 37–48.
7. Johnson, J.H.; Prejean, S.; Savage, M.K.; Townend, J. Anisotropy, repeating earthquakes, and seismicity associated with the 2008 eruption of Okmok volcano, Alaska. *J. Geophys. Res.-Sol. Earth* **2010**, *115*, B00B04.
8. Feuillet, N.; Beauducel, F.; Tapponnier, P. Tectonic context of moderate to large historical earthquakes in the Lesser Antilles and mechanical coupling with volcanoes. *J. Geophys. Res.-Sol. Earth* **2011**, *116*, B10308.
9. Jolly, A.D.; Neuberg, J.; Jeusset, P.; Sherburn, S. A new source process for evolving repetitious earthquakes at Ngauruhoe volcano, New Zealand. *J. Volcanol. Geoth. Res.* **2012**, *215*, 26–39.
10. Nonali, F.L.; Tibaldi, A.; Corazzato, C.; Tormey, D.R.; Lara, L.E. Quantifying the effect of large earthquakes in promoting eruptions due to stress changes on magma pathway: The Chile case. *Tectonophysics* **2013**, *583*, 54–67.
11. Hossain, K.M.A. Properties of volcanic pumice based cement and lightweight concrete. *Cem. Concr. Res.* **2004**, *34*, 283–291.
12. Páez-Flor, N.M.; Rubio-Hernández, F.J.; Velázquez-Navarro, J.F. Effect of various plasticisers on viscous flow properties of natural pozzolanic cement pastes. *Adv. Cem. Res.* **2020**, *32*, 20–29.
13. Schwartzentruber, A.; Catherine, C. Method of the concrete equivalent mortar (CEM)-a new tool to design concrete containing admixture. *Mater. Struct.* **2000**, *33*, 475–482.
14. Li, J.; Tan, D.; Zhang, X.; Wan, C.; Xue, G. Mixture design method of slef-compacting lightweight aggregate concrete based on rheological property and strength of mortar. *J. Build. Engin.* **2021**, *43*, 102660.
15. Arnaud, L.; Dierkens, M. Setting and hardening of cement based materials: Which differences between mortars and concretes? In *Advances in Construction Materials*; Gross, C.U., Ed.; Springer:Berlin/Heidelberg, Germany, 2007.
16. Rubio-Hernández, F.J.; Velázquez-Navarro, J.F.; Ordóñez-Belloc, L.M. Rheology of concrete: A study case based upon the use of the concrete equivalent mortar. *Mater. Struct.* **2013**, *46*, 587–605.
17. Ferraris, C.F.; Obla, K.H.; Hill, R. The influence of mineral admixtures on the rheology of cement paste and concrete. *Cem. Concr. Res.* **2001**, *31*, 245–255.
18. Larrard, F.; Sedran, T. Mixture-proportioning of high performance concrete. *Cem. Concr. Res.* **2002**, *32*, 1699–1704.
19. Flatt, R.J.; Larosa, D.; Roussel, N. Linking yield stress measurements: Spread test versus Viskomat. *Cem. Concr. Res.* **2006**, *36*, 99–109.

20. Mahaut, F.; Mokéddem, S.; Chateau, X.; Roussel, N.; Ovarlez, G. Effect of coarse particle volume fraction on the yield stress and thixotropy of cementitious materials. *Cem. Concr. Res.* **2008**, *38*, 1276–1285.
21. Newman, J. *Advanced Concrete Technology Set*; Elsevier: Amsterdam, The Netherlands, 2002.
22. Yammine, J.; Chaouche, M.; Guerinet, M.; Moranville, M.; Roussel, N. From ordinary rheology concrete to self-compacting concrete: A transition between frictional to hydrodynamic interactions. *Cem. Concr. Res.* **2008**, *38*, 890–896.
23. Lecompte, T.; Perrot, A.; Picandet, V.; Bellegou, H.; Amziane, S. Cement-based mixes: Shearing properties and pore pressure. *Cem. Concr. Res.* **2012**, *42*, 139–147.
24. Feys, D.; Verhoeven, R.; Schutter, G. Evaluation of time independent rheological models applicable to fresh selfcompacting concrete. *Appl. Rheol.* **2007**, *17*, 56244.
25. Saak, A.W.; Jenning, H.; Shah, S. New methodology for designing self-compacting concrete. *ACI Mater. J.* **2001**, *98*, 429–439.
26. Roussel, N. A theoretical frame to study stability of fresh concrete. *Mater. Struct.* **2006**, *39*, 81–91.
27. Kovler, K.; Roussel, N. Properties of fresh and hardened concrete. *Cem. Concr. Res.* **2011**, *41*, 775–792.
28. Shen, L.; Struble, L.; Lange, D. Modeling dynamic segregation of self-consolidating concrete. *ACI Mater. J.* **2009**, *106*, 375–380.
29. Larrard, F.; Ferraris, C.F.; Sedran, T. Fresh concrete: A Herschel-Bulkley material. *Mater. Struct.* **1998**, *31*, 494–498.
30. Cyr, M.; Legrand, C.; Mouret, M. Study of the shear-thickening effect of superplasticizers on the rheological behavior of cement pastes containing or not mineral additives. *Cem. Concr. Res.* **2000**, *30*, 1477–1483.
31. Feys, D.; Verhoeven, R.; Schutter, G. Fresh self-compacting concrete, a shear-thickening material. *Cement Concrete Res*. **2008**, *38*, 920–929.
32. *NTE INEN 490:2011*; Cementos hidráulicos compuestos. Instituto Ecuatoriano de Normalización: Quito, Ecuador, 2011. (In Spanish).
33. *NTE INEN 2380:2011*; Cementos hidráulicos. Requisitos de desempeño para cementos hidráulicos. Instituto Ecuatoriano de Normalización: Quito, Ecuador, 2011. (In Spanish).
34. *NTE INEN 196:2009*; Determinación de la finura mediante el aparato de permeabilidad al aire. Instituto Ecuatoriano de Normalización: Quito, Ecuador, 2009. (In Spanish).
35. *NTE INEN 156:2009*; Cemento hidráulico. Determinación de la densidad. Instituto Ecuatoriano de Normalización: Quito, Ecuador, 2009. (In Spanish).
36. Páez-Flor, N.M.; Rubio-Hernández, F.J.; Velázquez-Navarro, J.F. Steady viscous flow of some commercial Andean volcanic Portland cement pastes. *Adv. Cem. Res.* **2017**, *29*, 438–449.
37. Hammat, S.; Menadi, B.; Kenai, S.; Thomas, C.; Kirgiz, M.S.; de Sousa Galdino, A.G. The effect of content and fineness of natural pozzolana on the rheological, mechanical, and durability properties of self-compacting mortar. *J. Build. Eng.* **2021**, *44*, 103276.
38. Westerholm, M.; Lagerblad, B.; Silfwerbrand, J.; Forssberg, E. Influence of fine aggregate characteristics on the rheological properties of mortars. *Cem. Concr. Comp.* **2008**, *30*, 274–282.
39. De Schutter, G.; Pope, A.M. Quantification of the water demand of sand in mortar, *Constr. Build. Mater.* **2004**, *18*, 517–521.
40. *ASTM C 128:2007*; Standard Test Method for Density, Relative Density (Specific Gravity), and Absorption of Fine Aggregate. American Society for Testing and Materials: Philadelphia, PA, USA, 2007.
41. Roussel, N.; Ovarlez, G.; Garrault, S.; Brumaud, C. The origins of thixotropy of fresh cement pastes. *Cem. Concr. Res.* **2012**, *42*, 148–157.